CORE
Metadata, citation and similar papers at core.ac.uk
Provided by Edinburgh Research Explorer

THE UNIVERSITY of EDINBURGH

Edinburgh Research Explorer

Stone-Wales graphene: A Two Dimensional Carbon Semi-Metal with Magic Stability

Citation for published version:
Yin, H, Shi, X, He, C, Martinez-Canales, M, Li, J, Pickard, CJ, Tang, C, Ouyang, T, Zhang, C & Zhong, J 2019, 'Stone-Wales graphene: A Two Dimensional Carbon Semi-Metal with Magic Stability' Physical Review B: Condensed Matter and Materials Physics, vol. 99, no. 04, pp. 041405. DOI: 10.1103/PhysRevB.99.041405

Digital Object Identifier (DOI):
10.1103/PhysRevB.99.041405

Link:
Link to publication record in Edinburgh Research Explorer

Document Version:
Peer reviewed version

Published In:
Physical Review B: Condensed Matter and Materials Physics

General rights
Copyright for the publications made accessible via the Edinburgh Research Explorer is retained by the author(s) and / or other copyright owners and it is a condition of accessing these publications that users recognise and abide by the legal requirements associated with these rights.

Take down policy
The University of Edinburgh has made every reasonable effort to ensure that Edinburgh Research Explorer content complies with UK legislation. If you believe that the public display of this file breaches copyright please contact openaccess@ed.ac.uk providing details, and we will remove access to the work immediately and investigate your claim.

OPEN ACCESS

Download date: 09. May. 2019

Stone-Wales graphene: A Two Dimensional Carbon Semi-Metal with Magic Stability

HengChuang Yin[♯],[1,2] Xizhi Shi[♯],[1,2] Chaoyu He,[1,2,*] Miguel Martinez-Canales,[3,†] Jin Li,[1,2]
Chris J. Pickard,[4,5,‡] Chao Tang,[1,2] Tao Ouyang,[1,2] Chunxiao Zhang,[1,2] and Jianxin Zhong[1,2]

[1]*Hunan Key Laboratory for Micro-Nano Energy Materials and Devices, Xiangtan University, Hunan 411105, P. R. China;*
[2]*School of Physics and Optoelectronics, Xiangtan University, Xiangtan 411105, China.*
[3]*SUPA, School of Physics and Astronomy & CSEC, University of Edinburgh, Peter Guthrie Tait Road, Edinburgh EH9 3FD, United Kingdom*
[4]*Department of Materials Science & Metallurgy, University of Cambridge, 27 Charles Babbage Road, Cambridge CB3 0FS, United Kingdom*
[5]*Advanced Institute for Materials Research, Tohoku University 2-1-1 Katahira, Aoba, Sendai, 980-8577, Japan*

(Dated: January 11, 2019)

A two-dimensional carbon allotrope, Stone-Wales graphene, is identified in stochastic group and graph constrained searches and systematically investigated by first-principles calculations. Stone-Wales graphene consists of well-arranged Stone-Wales defects, and it can be constructed through a 90° bond-rotation in a $\sqrt{8}\times\sqrt{8}$ supercell of graphene. Its calculated energy relative to graphene, +149 meV/atom, makes it more stable than the most competitive previously suggested graphene allotropes We find that Stone-Wales graphene based on a $\sqrt{8}$ supercell is more stable than those based on $\sqrt{9}\times\sqrt{9}$, $\sqrt{12}\times\sqrt{12}$ and $\sqrt{13}\times\sqrt{13}$ super-cells, and is a "magic size" that can be further understood through a simple "energy splitting and inversion" model. The calculated vibrational properties and molecular dynamics of SW-graphene confirm that it is dynamically stable. The electronic structure shows SW-graphene is a semimetal with distorted, strongly anisotropic Dirac cones.

PACS numbers:

arXiv:1901.02966v1 [cond-mat.mtrl-sci] 9 Jan 2019

Elemental carbon adopts many different allotropes, including the three-dimensional (3D) cubic diamond, hexagonal diamond and graphite, the two-dimensional (2D) graphene[1] and graphynes[2], the one-dimensional (1D) nanotubes[3], as well as the zero-dimensional (0D) fullerenes[4], due to its ability to hybridize in sp, sp^2 and sp^3. Low-dimensional carbon materials, such as graphene and nanotubes, have attracted much scientific interest in view of their novel electronic and mechanical properties[1,5,6]. In particular, graphene is a well-known Dirac-cone material that exhibits high carrier mobility[1,5,6] and the quantum Hall effect[5,7,8] due to its semi-metallicity contributed from the active π-electrons[8,9]. The successes of isolating graphene[1,10,11] from graphite have spurred many efforts in searching for other 2D carbon allotropes beyond graphene. Graphynes[12,13] are alternative ways to fill the 2D space with mixed sp-sp^2 carbon atoms. They contribute rich electronic properties, including semiconductors, semi-metals and metals. Although graphynes with sp-hybridized bonding are energetically less stable than the pure sp^2-hybridized graphene, graphite and nanotubes, there are a few graphynes that have been experimentally synthesized[2,14].

The honeycomb-like graphene is not the only way to topologically fill 2D space with sp^2 hybridized carbon. Many other hypothetical graphene allotropes have been previously proposed. For example, the pentaheptites (R_{57-1} and R_{57-2}) containing exclusively 5-7 rings proposed in 1996[15] and 2000[16,17], the Haeckelite sheets (H_{567} and O_{567}) proposed by Terrones[17], the low-energy ψ-graphene previously proposed by Csányi[18] and recently investigated by Li[19], the dimerites (dimerite I, II and III with metallic property) and octites (metallic octite M_1, M_2, M_3 and semiconducting octite SC) constructed through defects patterns[20–23], the biphenylene sheets (New-W and New-C) containing 4-6-8 rings[24,25], the T-graphene containing 4-8 rings[26–28], the PO-graphene containing 5-8 rings (OPG-L and OPG-Z)[29,30], the graphene superlattice structures (including pza-C_{10})[31], the 187-C_{65}, 191-C_{63} and 127-C_{41} sheets[32], the 5-6-8 rings HOP-graphene[33], δ-graphene[34] and pentahexoctite[35], as well as the recently proposed phagraphene[36]. Most of these 2D carbon allotropes are more energetically stable than the experimentally viable graphynes[2,14] and C_{60}[4]. In particular, the most stable ψ-graphene[8] and phagraphene[36] possess energies just about 165 meV/atom and 201 meV/atom higher than that of graphene, and might be synthesized in future experiments.

Previously suggested 2D carbon allotropes, other than octite SC[23], have less than 20 atoms per cell. In this work, we have performed stochastic group and graph-constrained searches for 2D carbon allotropes with up to 24 atoms per unit cell. Graph-constrained searches have been performed using our recently developed RG^2 code[37]. Structural details, energetics and properties have all been computed using density functional theory (DFT) and the PBE exchange-correlation functional[41] as implemented in Vienna Ab-initio Simulation Package (VASP)[38]. Carbon was modelled with a $2s^2\,2p^2$ PAW potential[39,40] and the energy cutoff was set to be 500 eV. The Brillouin Zone (BZ) sampling meshes were denser than 0.21 Å^{-1} to ensure the convergence. The vibrational spectrum of SW-graphene was computed using the phonopy code[42].

Our RG^2 searches produced nearly all the previously proposed 2D carbon allotropes. It further identified 33 previously unreported competitive structures as shown in Fig. ref-fig1, including the most stable allotrope known to date. Its structure contains well arranged Stone-Wales defects (SWD, 5577-ring segments)[43–45] on a $\sqrt{8}$ graphene supercell, and we call it Stone-Wales graphene (SW-graphene hereafter). SW-graphene, inserted in Fig. 1, has 16 carbon atoms and one SWD in its primitive unit cell. The SWDs periodically connect to each other with six-fold carbon rings boundary. As

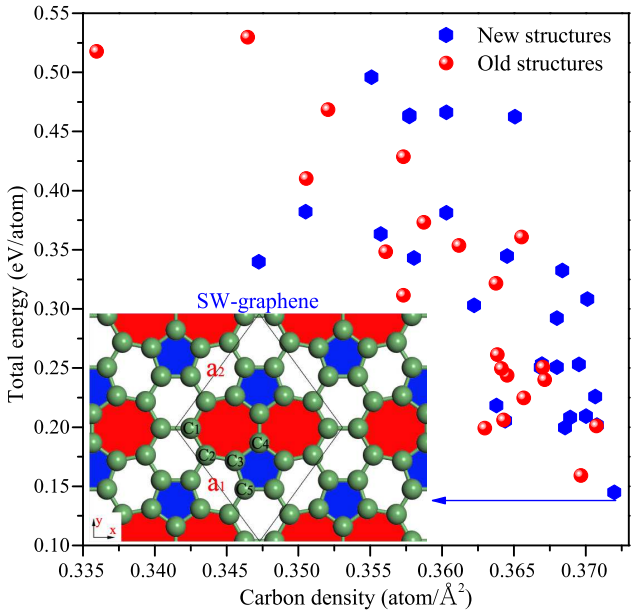

FIG. 1: Calculated energies (relative to graphene) and carbon densities of the new discovered (blue hexagon) and previously proposed (red balls) graphene allotropes with energy relative to graphene less than 550 meV per atom. *Inset:* The crystalline view of the most stable one (SW-graphene) with symmetry of *Cmmm*, showing its topological pattern containing five-, six- and seven-fold carbon rings.

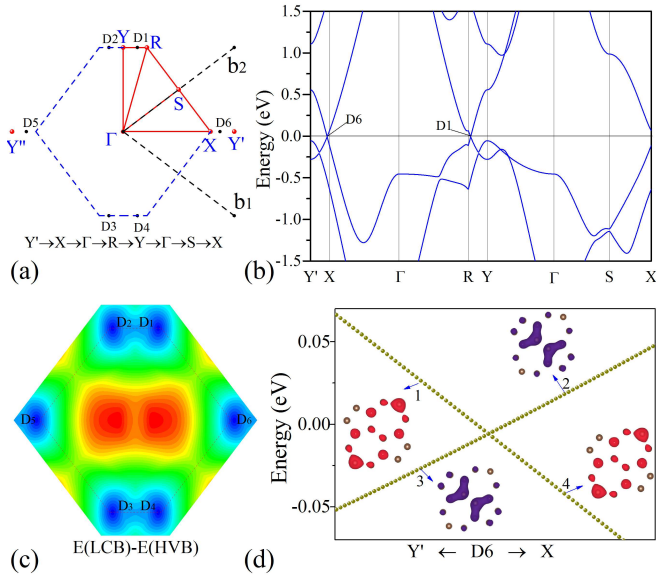

FIG. 2: The first Brillouin zone (BZ) (a), the band structures (b), the 2D color mapping of the energy differences between LCB and HVB (c), as well as the band decomposed charge density distributions of SW-graphene (d).

indicated in Fig. 1, the primitive cell (with optimized lattice constants of a=b=6.683 Å, c=12.00 Å and γ =105.779°) of SW-graphene contains 5 inequivalent carbon atoms C_1, C_2, C_3, C_4 and C_5, located at positions 4h (0.09, 0.09, 0.5), 8q (0.299, 0.062, 0.5), 8q (0.497, 0.211, 0.5), 4j (0.564, 0.435, 0.5) and 4j (0.682, 0.143, 0.5), respectively. The bond lengths (1.378-1.458 Å) and bond angles (106.11-133.95°)[46] in SW-graphene are very close to those in ideal graphene, which indicate that it should be a low-lying 2D carbon allotrope.

We calculated the energies of the new discovered and previously proposed graphene allotropes[46]. Those with energy relative to graphene less than 550 meV/atom are shown in Fig. 1. The most stable three graphene allotropes previously proposed, ψ-graphene[18,19], octite M_1[22] and phagraphene[36], lie 159, 199 and 201 meV/atom above graphene, respectively. The relative energy of SW-graphene is +149 meV/atom, which indicates that it is energetically more favorable than either. We notice that the carbon density of SW-graphene (0.372 atom/Å^2) is also comparable to that of graphene (0.379 atom/Å^2), larger than all the previously proposed 2D carbons.

With its remarkable energetic stability, SW-graphene might be synthesized if it is dynamically stable. The phonon dispersion bands and phonon density of states of SW-graphene show no imaginary frequency mode in the whole Brillouin Zone[46], indicating SW-graphene is dynamically stable. *Ab initio* NVT molecular dynamics on a 3×3 supercell and a timestep of 1 fs confirm that SW-graphene is dynamically stable at 300 K for at least 5 ps. No structural changes occur, with the only distortion being thermal oscillations of atoms near their equilibrium positions (Fig. S3 in the supplemental material[46]). That is to say, SW-graphene should be stable at room temperature.

As discussed in previous literatures concerning the synthesis of ψ-graphene[18] and Phagraphene[36], defect topology[44,49] and molecular assembly[47,50] are two potential routes to synthesize SW-graphene. We notice that SW-graphene can be decomposed as ethylene and benzene (or cyclopentene and propylene) as indicated in Fig. S3. That is to say, catalyzer-associated assembly of ethylene and benzene (or cyclopentene and propylene) on a proper substrate could be a way to synthesize SW-graphene.

Most of the previously proposed graphene allotropes, such as ψ-graphene[18,19] and octite M_1[22] are metallic. A few of them have been reported as semiconductors and semimetals, such as octite SC[23] and Phagraphene[36]. Our calculations show that SW-graphene is a semi-metal with distorted Dirac-cones. There are two equivalent Dirac-cones in its first Brillouin zone (BZ) as indicated in Fig. 2 (a). The calculated band structure of SW-graphene along the pathway of Y'–X–Γ–R–Y–Γ–S–X is shown in Fig. 2 (b). A symmetry analysis shows that, along Y'–Γ, at least one band must cross the Fermi energy (D_6). We can see that there is a Dirac-point located at the point (D_1) between R–Y. The calculated density of states (DOS) at Fermi-level is zero, which confirms that such a Dirac-point is not formed by band-folding. Fig. 2 (c) shows the energy difference between the highest valance band (HVB) and the lowest conduction band (LCB). We can see that there are six zero points (Dirac-points) within that region. D_2 is equivalent to D_1 due to mirror symmetry along *y*-axis. D_6 (D_5) is equivalent to D_2 (D_1) via a reciprocal lattice vector shift of b_1 (negative b_2) as indicated in Fig. 2 (a). D_4 and D_3 are equivalent to D_1 and D_2, respectively, due to the mirror symmetry on *x*-axis.

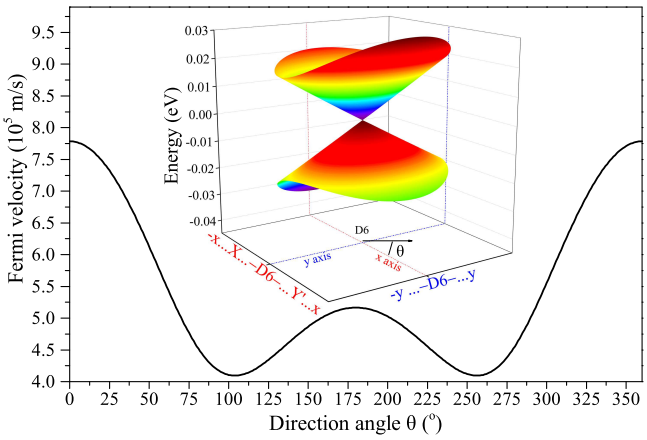

FIG. 3: The 3D plot of the Dirac-cone formed by the highest valence band (HVB) and the lowest conduction band (LCB) in the vicinity of the Dirac point (D_6) and the corresponding direction-dependent Fermi velocities for Fermions in SW-graphene.

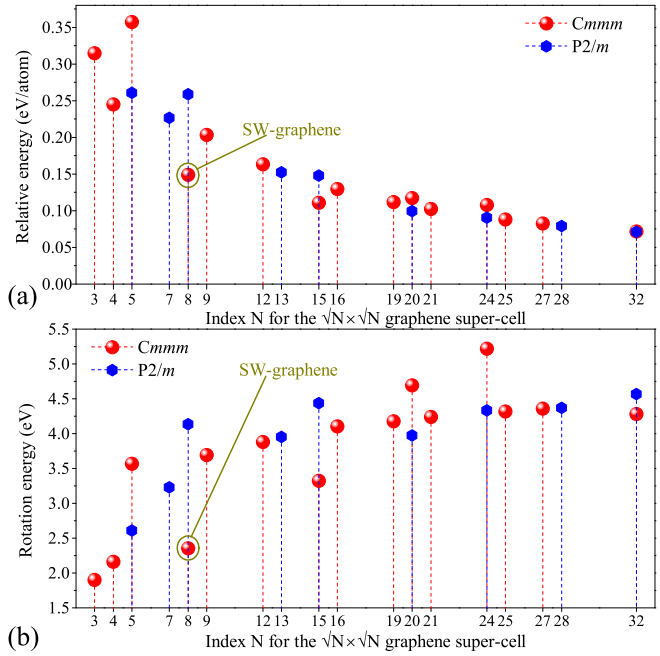

FIG. 4: Relative energies *(a)* and SWD rotation energies ($E_{\sqrt{N}} - NE_{\text{graphene}}$) (b) of $\sqrt{N}\times\sqrt{N}$ graphene super-cells with a single SWD. SW-graphene corresponds to $N = 8$. Red balls denote structures that adopt *Cmmm* symmetry; blue hexagons denote structures adopting $P2/m$ symmetry.

To further understand the formation of the Dirac-cones in SW-graphene, the band-decomposed charge density distributions of the four points (1, 2, 3, 4) near the Dirac-point D_6 are investigated. As shown in Fig. 2 (d), we can see that the charge densities of points 1 and 4 are very similar to each other. Those for points 2 and 3 also appear in same distribution. This indicates that the Dirac-points in SW-graphene are formed by band-cross similar to those in phagraphene[36].

To show the cone-like feature of these Dirac-points, the 3D surface band structures of the HVB and LCB near D6 are plotted. As inserted in Fig. 3, the HVB and LCB cross each other at point D_6 and form a distorted Dirac-cone with obvious anisotropicity. Based on the calculated surface band structures, we then investigated the direction-dependent Fermi velocities of the Fermions in cone D_6 as shown in Fig. 3. The corresponding Fermi velocities are given by $\upsilon_f = \mathrm{E(k)}/\hbar|k|$. Our calculated Fermi velocities of Phagraphene along x, y and $-y$ directions are 6.54×10^5 m/s, 6.34×10^5 m/s and 4.17×10^5 m/s, respectively. The largest and smallest Fermi velocities in graphene are 8.26×10^5 m/s and 7.74×10^5 m/s, respectively. These results are consistent with those reported before[36]. However, we find that the largest Fermi velocity in phagraphene is not the 6.54×10^5 m/s along the x direction. It is about 7.02×10^5 m/s along the $\pi/6$ direction, which was not reported in previous literature[36].

The result in Fig. 3 shows that the Fermi velocities of SW-graphene along the x ($\theta = 0°$), $-x$ ($\theta = 180°$) and y ($\theta = 90°$) directions are 7.78×10^5 m/s, 5.16×10^5 m/s and 4.25×10^5 m/s, respectively. Fermions in SW-graphene along the x direction possesses the largest velocity of 7.78×10^5 m/s. Along the direction of $\theta\approx7\pi/12$, the Fermi velocity (4.09×10^5 m/s) is the smallest. These results indicate that SW-graphene possesses anisotropic electronic properties similar to phagraphene[36], which are more obvious than those in graphene.

We have also computed the band structure using maximally-localized Wannier functions using Quantum-Espresso[51] and Wannier90[52]. Our starting guess has been p_z orbitals on each atom, sp^2 orbitals on alternating atoms where possible, and σ-bonds on the remaining bonds. This replicates the DFT bands up to at least 4 eV above the Fermi energy[46]. Projecting into orbitals show a picture similar to graphene: the low-lying bands come from sp^2 orbitals, while the bands near Fermi energy can be described by p_z interactions. The result of such a projection is shown in Fig. S6. This opens up the creation of an effective Hamiltonian for SW-graphene, but even a nearest-neighbour model has 15 symmetry-independent hopping parameters. The Berry phase around a Dirac cone takes a nontrivial value of π.

SW-graphene can be understood as a simple 90° carbon bond rotation[46]. However, we show now the stability of SW-graphene is not just the result of a single defect in a supercell, and that SW-graphene is a structure in its own right. Fig. 4 (a) shows the energies of $\sqrt{N}\times\sqrt{N}$ graphene supercells with a single SWD. Larger cells are more stable, as expected, despite relaxation in smaller cells reducing a large fraction of the rotation energy penalty of a SWD. However, SW-graphene ($\sqrt{8}$-*Cmmm*) is 50 meV/atom more stable than $N = 9$ and, unexpectedly, more stable than $N < 15$. The rotation energy in SW-graphene is almost as low as for the $N = 3, 4$ cases. This suggests $N = 8$ is a *"magic size"*, followed by other two magic sizes of $\sqrt{15}$ and $\sqrt{20}$.

A simple "energy splitting and inversion" model is used to understand the "magic stability" of SW-graphene as shown in Fig. 5. After bond-rotation, we compare the energies and rotation energies of $\sqrt{7}$, $\sqrt{8}$-*Cmmm*, $\sqrt{8}$-$P2/m$, $\sqrt{9}$, $\sqrt{12}$ and

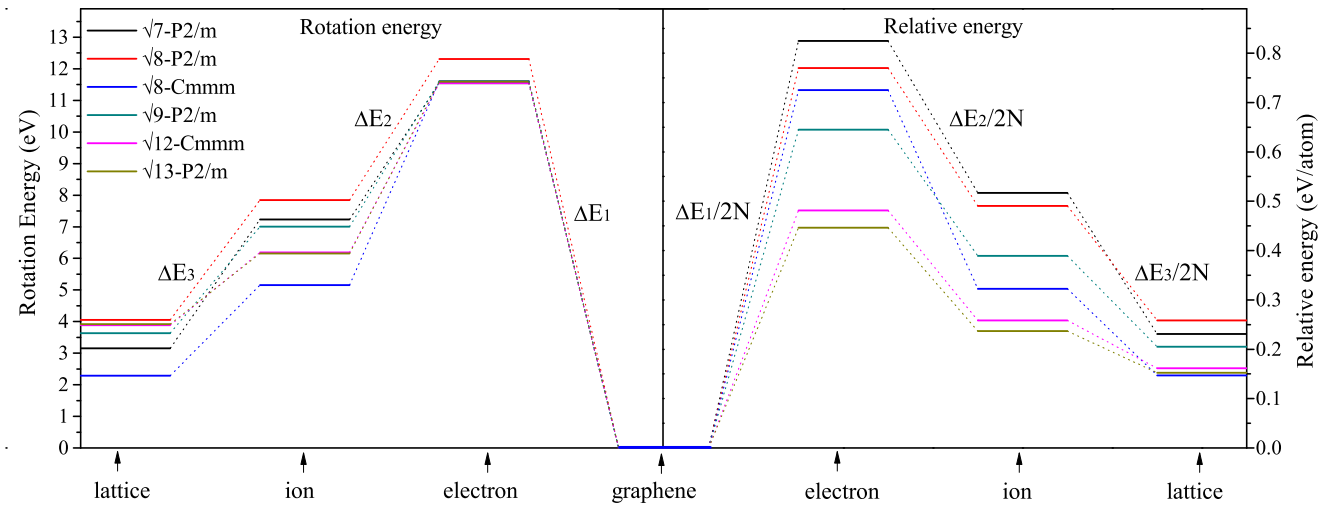

FIG. 5: Energy splitting and inversion model (left: rotation energies eV per cell; right: relative energies eV/atom relative to graphene) based on the comparison of energy changes between $\sqrt{7}$, $\sqrt{8}$-*Cmmm*, $\sqrt{8}$-$P2/m$, $\sqrt{9}$, $\sqrt{12}$ and $\sqrt{13}$ in three steps after bond-rotation, namely, electronic minimization in fixed configuration (electron), ionic relaxation (ion), as well as full lattice and ionic relaxation (lattice).

$\sqrt{13}$ in three steps: electronic minimization in fixed configuration, ionic relaxation, as well as full lattice and ionic relaxation. In fixed configuration, other than an obvious energy penalty for $\sqrt{8}$-$P2/m$, other candidates show roughly the same ΔE_1. The averaged values $\Delta E_1/2N$ split or reverse the energy positions of $\sqrt{7}$, $\sqrt{8}$-*Cmmm*, $\sqrt{8}$-$P2/m$, $\sqrt{9}$, $\sqrt{12}$ and $\sqrt{13}$. After bond-rotation, the defected atoms[53] in the system adjust their position to minimize the energy. With larger ratio of defected atoms, ionic and lattice relaxations release more energy ΔE_2 and ΔE_3 in small cells ($\sqrt{7}$, $\sqrt{8}$-*Cmmm*, $\sqrt{8}$-$P2/m$) than larger systems ($\sqrt{9}$, $\sqrt{12}$ and $\sqrt{13}$). The results in Fig. 5 show how $\sqrt{8}$-*Cmmm* releases the largest amount of energy on ionic relaxation, which is eventually the cause of the stability of SW-graphene.

We finally check if Dirac-cones are common features in the SW-graphene allotropes family[46]. SW-graphene allotropes $\sqrt{3}$, $\sqrt{4}$, $\sqrt{5}$-*Cmmm*, $\sqrt{7}$, $\sqrt{9}$, $\sqrt{12}$ and $\sqrt{15}$-*Cmmm* are all metallic. Those named as $\sqrt{5}$-$P2/m$, $\sqrt{8}$-$P2/m$, $\sqrt{13}$, $\sqrt{15}$-$P2/m$, $\sqrt{19}$, $\sqrt{20}$-*Cmmm*, $\sqrt{20}$-$P2/m$, $\sqrt{21}$, $\sqrt{24}$-$P2/m$, $\sqrt{28}$ and $\sqrt{32}$-$P2/m$, are semiconductors with direct or indirect band gaps. Only a few of them are semi-metals featuring Dirac-cones: $\sqrt{8}$-*Cmmm* (SW-graphene), $\sqrt{16}$, $\sqrt{24}$-*Cmmm*, $\sqrt{25}$, $\sqrt{27}$ and $\sqrt{32}$-*Cmmm*.

In summary, a 2D carbon allotrope is discovered using our recently developed RG^2 code. It is named SW-graphene in view of its structural feature consisting of the well-known Stone-Wales defects. The calculated total energy shows that SW-graphene is energetically more favorable than the previously proposed phagraphene and ψ-graphene. It is also confirmed to be a dynamically stable carbon phase according to its phonon dispersion and molecular dynamics. The calculated band structures shows that SW-graphene is a semimetal with distorted Dirac-cones, containing Fermions with direction-dependent Fermi velocities. In view of its remarkable stability and novel properties, SW-graphene is a desirable target for future synthesis. A family of SW-graphene allotropes constructed through 90°-rotation of carbon-bonds in given $\sqrt{N}\times\sqrt{N}$ graphene super-cells are investigated. We find that $\sqrt{8}$-*Cmmm* SW-graphene is an interesting system with "magic stability" and not all the SW-graphene allotropes are semi-metallic like $\sqrt{8}$-*Cmmm* SW-graphene. The "magic stability" of $\sqrt{8}$-*Cmmm* SW-graphene is further discussed based on a theoretical "energy splitting and inversion" model.

This work is supported by the National Natural Science Foundation of China (Grants No. 11704319, No. 11647063, No. A040204, and No. 11204261), the National Basic Research Program of China (No. 2015CB921103), the Natural Science Foundation of Hunan Province, China (Grant No. 2016JJ3118), and the Program for Changjiang Scholars and Innovative Research Team in University (No. IRT13093). MMC is grateful for computational support from the UK Materials and Molecular Modelling Hub, which is partially funded by EPSRC (EP/P020194), for which access was obtained via the UKCP consortium and funded by EPSRC grant EP/P022561/1. C. J. P. is supported by the Royal Society through a Royal Society Wolfson Research Merit award.

* Electronic address: hechaoyu@xtu.edu.cn
† Electronic address: miguel.martinez@ed.ac.uk
‡ Electronic address: cjp20@cam.ac.uk

[1] K. S. Novoselov, A. K. Geim, S. V. Morozov, D. Jiang, Y. Zhang, S. V. Dubonos, I. V. Grigorieva, and A. A. Firsov, Science, 306, 666 (2004).

[2] G. Li, Y.Li, H. Liu, Y. Guo, Y. Li, and D. Zhu, Chem. Commun., 46, 3256 (2010).
[3] S. lijima, Nature(London), 354, 56 (1991).
[4] H. W. Kroto, J. R. heath, S. C. Obrien, R. F. Curl, and R. E. Smaliey, Nature(London) 318, 162 (1985).
[5] Y. Zhang, Y. -W. Tan, H. L. Stormer, and P. Kim, Nature, 438,201 (2005).
[6] K. I. Bolotin, F. Ghahari, M. D. Shulman, H. L. Stormer, P. Kim, Nature, 462, 196 (2009).
[7] K. S. Novoselov, Z. Jiang, Y. Zhang, S. V. Morozov, H. L. Stormer, U. Zeitler, J. C. Maan, G. S. Boebinger, P. Kim, and A. K. Geim, Science, 315, 5817 (2007).
[8] K. S. Novoselov, E. McCann, S. V. Morozov, V. I. Fal'ko, M. I. Katsnelson, U. Zeitler, D. Jiang, F. Schedin , and A. K. Geim, Nat. Phys., 2, 177 (2006).
[9] C. L. Kane and E. J. Mele, Phys. Rev. Lett.,95, 226 (801).
[10] K. S. Kim, Y. Zhao, H. Jang, S. Y. Lee, J. M. Kim, K. S. Kim, J. H. Ahn, P. Kim, J. Y. Choi and B. H. Hong, Nature, 457, 706 (2009).
[11] Z. Z. Sun, Z. Yan, J. Yao, E. Beitler, Y. Zhu, J. M. Tour, Nature, 468, 549 (2010).
[12] R. H. Baughman, and H. Eckhardt, J. Chern. Phys., 87, 6687 (1987).
[13] N. Narita, S. Nagai, S. G. Suzuki, and K. J. Nakao, Phys. Rev. B, 58, 11009 (1998).
[14] R. Matsuoka, R. Sakamoto, K. Hoshiko, S. Sasaki, H. Masunaga, K. Nagashio, and H. Nishihara, J. Am. Chem. Soc., 139, 3145 (2017).
[15] V. H. Cresspi, L. X. Benedict, M. L. Cohen, and S. G. Louie, Phys. Rev. B, 53, R13303 (1996).
[16] M. Deza, P. W. Fowler, M. Shtogrin, and K. Vietze, J. Chem. Inf. Comput. Sci., 40, 1325 (2000).
[17] H. Terrones, M. Terrones, E. Hernández, N. Grobert,J-C. Charlier, and P. M. Ajayan, Phys. Rev. Lett., 84, 1716 (2000).
[18] C. Csányi, C. J. Pickard, B. D. Simons, and R. J. Needs, Phys. Rev. B, 75, 085432 (2007).
[19] X. Y. Li, Q. Wang, and P. Jena, J. Phys. Chem. Lett.,8, 3234 (2017).
[20] M. T. Lusk, and L. D. Carr, Phys. Rev. Lett., 100, 175503 (2008).
[21] M. T. Lusk, and L. D. Carr, Carbon, 47, 2226 (2009).
[22] D. J. Appelhans, L. D. Carr, and M. T. Lusk, New. J. Phys., 12, 125006 (2010).
[23] D. J. Appelhans, Z. B. Lin, and M. T. Lusk, Phys. Rev. B, 82, 073410 (2010).
[24] M. A. Hudspeth, B. W. Whitman, V. Barone, and J. E. Peralta, ACS nano.,4, 4565 (2010).
[25] X. Q. Wang, H. D. Li, and J. T. Wang, Phys. Chem. Chem. Phys., 15, 2024 (2013).
[26] J. Nisar, X. Jiang, B. Pathak, J. J. Zhao, T. W. Kang, and R. Ahuja, Nanotechnology, 23, 385704 (2012).
[27] X. Q. Wang, H. D. Li, and J. T. Wang, Phys. Chem. Chem. Phys., 14, 11107 (2012).
[28] Y. Liu, G. Wang, Q. S. Huang, L. W. Guo, and X. L. Chen, Phys. Rev. Lett., 108, 225505 (2012).
[29] C. P. Tang, and S. J. Xiong, AIP adv., 2, 042147 (2012).
[30] C. Su, H. Jiang, and J. Feng, Phys. Rev. B, 87, 075453 (2013).
[31] X. G. Luo, L. M. Liu, Z. P. hu, W. H. Wang, W. X. Song, F. F. Li, S. J. Zhao, H. Liu, H. T. Wang, and Y. J. Tian, J. Phys. Chem. Lett., 3, 3373 (2012).
[32] H. G. Lu, and S. D. Li, J. Mater. Chem. C, 1, 3677 (2013).
[33] B. Mandal, S. Sarkar, A. Pramanik, and P. Sarkar, Phys. Chem. Chem. Phys., 15, 21001 (2013).
[34] X. Y. Fan, J. Li, and G. Chen, RSC Adv., 7, 17417 (2017).
[35] B. R. Sharma, A. Manianath, and A. K. Singh, Sci. Rep., 4, 7164 (2014).
[36] Z. H. Wang, X. F. Zhou, X. M. Zhang, Q. Zhu, H. F. Dong, M. W. Zhao, and A. R. Oganov, Nano Lett., 15, 6182 (2015).
[37] X. Z. Shi, C. Y. He, C. J. Pickard, C. Tang, and J. X. Zhong, Phys. Rev. B, 97, 014104 (2018).
[38] G. Kresse, and J. Furthmüller, Phys. Rev. B, 54, 11169 (1996).
[39] P. E. Blöchl, Phys. Rev. B, 50, 17953 (1994).
[40] G. Kresse, and D. Joubert, Phys. Rev. B, 59, 1758 (1999).
[41] J. P. Perdew, K. Burke, and M. Ernzerhof, Phys. Rev. Lett., 77, 3865 (1996).
[42] Phonopy: http://atztogo.github.io/phonopy/
[43] A. J. Stone and D. J. Wales, Chem. Phys. Lett. 128, 501(1986).
[44] J. Kotakoski, A. V. Krasheninnikov, U. Kaiser, and J. C. Meyer, Phys. Rev. Lett., 106, 105505 (2011).
[45] J. Ma, D. Alfe, A. Michaelides, and E. G. Wang, Phys. Rev. B, 80, 033407 (2009).
[46] See supplemental material containing additional discussions about structures, stabilities and electronic properties at **URL**.
[47] J. V. Barth, G. Costantini and K. Kern, Nature, 437, 671 (2005).
[48] G. Schusteritsch, and C. J. Pickard, Phy. Rev. B, 90, 035424 (2014).
[49] J. Lahiri, Y. Lin, P. Bozkurt, I. I. Oleynik and M. Batzill, Nat. Nanotechnol., 5, 326 (2010).
[50] L. Grill, M. Dyer, L. Lafferentz, M. Persson, M. V. Peters and S. Hecht, Nat. Nanotechnol. 2, 687 (2007).
[51] P. Giannozzi et al, J. Phys.: Condens. Matter, 29, 465901 (2017).
[52] A. A. Mostofi, J. R. Yates, G. Pizzi, Y. S. Lee, I. Souza, D. Vanderbilt and N. Marzari, Comp. Phys. Commun., 185, 2309 (2014).
[53] Defected atoms are the selected two atoms (bond) and their four surroundings. The ratio of defected atoms is defined as (2+4)/2N, in which 2 and 4 denotes the selected two atoms and the four surroundings, respectively. 2N is the total atoms number in the cell. For example, the ratio for SW-graphene with size of $\sqrt{8}$ and $\sqrt{32}$ are 6/16 and 6/64, respectively.